Authentication-based on Biomechanics of Finger Movements captured using Optical Motion-Capture

Brittany Lewis, Christopher J. Nycz, Gregory S. Fischer, and Krishna K. Venkatasubramanian

Worcester Polytechnic Institute, Worcester MA 01609, USA
{bfgradel,cjnycz,gfischer,kven}@wpi.edu

Abstract. In this paper, we propose an authentication approach based on the uniqueness of the biomechanics of finger movements. We use an optical-marker-based motion-capture as a preliminary setup to capture goniometric (joint-related) and dermatologic (skin-related) features from the flexion and extension of the index and middle fingers of a subject. We use this information to build a personalized authentication model for a given subject. Analysis of our approach using finger motion-capture from 8 subjects, using reflective tracking markers placed around the joints of index and middle fingers of the subjects shows its viability. In this preliminary study, we achieve an average equal error rate (EER) — when false accept rate and false reject rate are equal — of 6.3% in authenticating a subject immediately after training the authentication model and 16.4% ERR after a week.

Keywords: Authentication · Biometrics · Finger Biomechanics · Motion-capture

1 Introduction

The idea behind biometrics is to use, in an automated manner, the *traits* of human physiology and/or behavior as a way to uniquely recognize (authenticate) a person and clearly distinguish this person from others. Biometric data are increasingly being used in a large number of governmental and private programs, such as airport security, school attendance, and public assistance programs [9]. The increase in the use of biometric data to control access to programs, services, and facilities raises the need for newer biometric modalities. Once we have linked an identity to a set of biometric traits collected from a person, we can then identify and/or authenticate them as well.

In this paper, we make the case for a novel biometric-based authentication approach that uses biometric traits from human fingers. Human fingers are extremely complex limbs. The way the fingers of a person move to bend (flexion), straighten (extension) and rotate (circumduction) is determined by their anatomy. That is, the combination of the ligaments, blood vessels, joints, bone structure, tissues, muscle, and skin that constitute fingers determine the type and extent of movements they make. We argue that by using notions from biomechanics we can capture these anatomical characteristics from a person's fingers and develop a rich new class of traits, which can be used as biometrics. Of course, finger-based biometrics is nothing new. Biometrics based on fingerprints

[10], palm print [8], finger vein patterns [12], and even knuckle-print [5] have existed for a while. As important as these biometrics are, we argue that there is a whole slew of finger-centric biometrics that have not yet been explored, those based on the uniqueness of the *biomechanics of a person's* fingers. Finger biomechanics has many uses as a complementary biometric for people for whom existing biometrics fail. For example, the visually impaired. Fewer than 10% of people who are legally blind in the US are able to read Braille, they cannot easily use ubiquitous PIN/password-based authentication systems [3]. Hence, a solution based on biomechanics can be very useful for such a population.

In order to capture the biomechanics of a person's fingers, we explore an approach that uses marker-based optical motion-capture of the flexion and extension of a person's index and middle fingers to understand the unique patterns underlying such motion. We then build a machine learning-based *authentication model* that uses ensemble learning and subject-specific features, to capture the individual uniqueness of the finger flexions and extensions. This model can then be used to identify a person when they perform a single finger flexion and extension at a later time. Although we use motion capture to identify the key characteristics in this preliminary study due to the high precision and frame rate, ultimately these features are expected to be able to be identified using compact and economical sensors.

In this preliminary work, we use marker-based motion-capture to demonstrate the viability of finger biomechanics as a biometric for authentication. Analysis of our approach using finger motion-capture from 8 subjects, using reflective tracking markers placed around the joints of index and middle fingers, shows an average equal error rate (EER)[1] of $\sim 6.3\%$ in authenticating an individual immediately after training and around 16.4% EER after a week. The **contributions** of this work are: (1) a preliminary authentication approach based on biometrics derived from finger movement captured using a motion-capture system, (2) demonstration of the viability of the proposed approach using finger movement data collected longitudinally. Note that, in this work, we only aim to show the viability of the finger biomechanics as a biometric. There are several problems that still need to be addressed to make an authentication system that uses finger biomechanics, for instance, eliminating the need for markers in the motion capture, which we plan to consider in the future.

1.1 Problem Statement

We next detail our problem statement and the assumed threat model for this work. The principal problem that we address in this paper is *to determine if the flexion and extension of index and middle fingers of a subject are capable of uniquely identifying them.* We assume that the threat to our authentication approach comes from adversaries trying to declare themselves to be a particular subject (i.e., victim) and try to use their own finger movements to authenticate as the victim. For the purposes of this work, we assume that adversaries: (1) do not have access to the authentication model, and (2) cannot pollute the authentication model during the training stage.

[1] Equal error rate is the value where the false accept and false reject rates for a model are equal.

2 Approach

Our approach to authentication based on flexion and extension of a person's fingers has four phases. *Data collection phase* describes our process for capturing a subject's index and middle finger flexion and extension using a marker-based motion-capture setup. The *feature extraction phase* then processes this motion-capture data to extract several biomechanical traits of the fingers. We then use these features to train an authentication model in the *training phase*. Finally, in the *authentication phase*, we used the authentication model to identify the subject at a later time. We now describe each of these phases in detail.

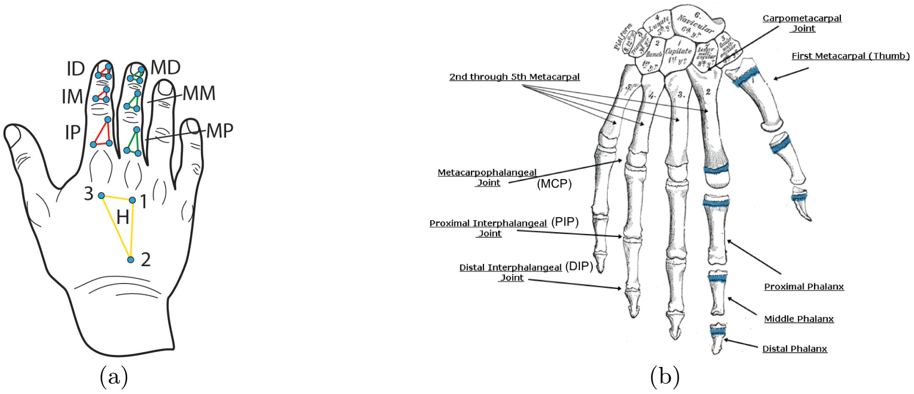
ID
MD
IM
MM
IP
MP
3
1
H
2
(a)
Carpometacarpal Joint
First Metacarpal (Thumb)
2nd through 5th Metacarpal
Metacarpophalangeal Joint (MCP)
Proximal Interphalangeal (PIP) Joint
Distal Interphalangeal (DIP) Joint
Proximal Phalanx
Middle Phalanx
Distal Phalanx
(b)

Fig. 1. An illustration of: (a) motion-capture marker placement and naming convention used for data collection, (b) reference for various joints in the hand. In (a) D, M, P, and H stand for distal, medial, proximal, and hand, respectively. While I and M stand for index and middle, respectively.

2.1 Motion-Capture-based Data Collection

We collected data from 8 different subjects. Each subject had 21 reflective hemispherical markers (3mm facial markers, NaturalPoint, Inc., Corvallis Oregon) [2] attached to the dorsum of their right hand using a cosmetic adhesive. We placed three markers over each presumed rigid segment of the index and middle fingers, establishing a 3DoF reference frame for each. No articulation (movement) is assumed to occur between the 2nd and 3rd metacarpal bones, hence a single set of three markers is placed over them, establishing the hand tracking frame H. The marker placement and their naming convention is shown in Figure 1 (a). Figure 1 (b) shows the various joints in the hand for reference. We asked the participants to sit at a table with 8 optical tracking cameras (Optitrack Flex 13, NaturalPoint, Inc.,) placed to the left, right, front, and above the hand. We placed the cameras approximately 1m from the center of the capture volume. Prior to data collection, for each subject, we calibrated the cameras with a 100mm long calibration wand until an average residual error of less than 0.3mm was achieved. Position data for the markers, relative to a global reference frame, was logged at 120Hz. Markers were manually labeled in post-processing (we expect to automate this in the future).

Each subject was instructed to repeatedly perform flexion and extension within the motion-capture volume for both index and middle fingers. This results in 4 types of joint movements for flexion: (1) coupled flexion of the proximal

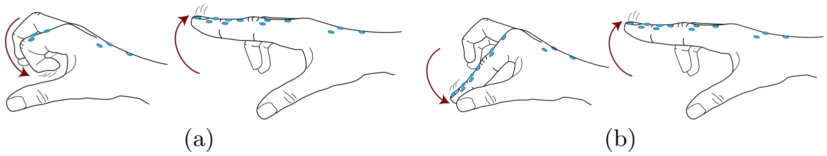

Fig. 2. An illustration of a set of performed movements for the index finger and its markers: (a) Coupled flexion and extension of the proximal interphalangeal (PIP) and distal interphalangeal (DIP) joints. (b) Flexion and extension of the metacarpophalangeal (MCP) joint.

interphalangeal (PIP) and distal interphalangeal (DIP) joints of the *index finger*, (2) flexion of the *index finger* metacarpophalangeal (MCP) joint, (3) coupled flexion of the proximal interphalangeal (PIP) and distal interphalangeal (DIP) joints of the *middle finger*, and (4) flexion of the *middle finger* metacarpophalangeal (MCP) joint. A depiction of these movements for the index finger is shown in Figures 2 (a) and 2 (b). Since every flexion is accompanied by an extension of the finger, we have the same 4 types of joint movements for extension as well. We demonstrated the finger movement to the participants before data collection. Even though, we ask the users to perform simple finger flexions and extensions, the exact angle of flexion/extension is not prescribed or controlled. We aim to build aggregate models characterizing the overall flexion/extension capability of the user based on a variety of characteristics (see next section), which turn out to be unique. For example, Figure 3 shows the joint positions for the index fingers of 2 different subjects while they repeatedly flex their MCP. The viewpoint is set be orthogonal to the MCP axes of both subjects and their MCPs are fixed at 0,0. Their fingers are fully extended when the joints are near the line x=0. It is easy to see that the joints for the two subjects follow distinct paths. Once the data was collected, we post-processed it to calculate the position and orientation of each joint throughout the performed finger movement. The positions and orientations of the joints were found from the motion-capture data using methods of Gamage et al. [7].

2.2 Feature Extraction

For feature extraction, we considered not just the joints specifically being flexed, but rather all the joints of the index and middle fingers. Biomechanic and neurological features, such as muscle synergies and friction between adjacent tendons, typically prohibit decoupled movement of the fingers. These coupled movements may contain difficult-to-replicate signatures specific to an individual. For each of the two tracked fingers, there were 58 features captured which can be divided into two categories: (1) *goniometric features*, which describe joint rotations, and (2) *dermatologic features*, which describe skin movement. There were 48 goniometric and 10 dermatological features.

To define the start and end time of a flexion motion, we consider the point where the joint reaches 10% of its range of motion as the start and the point at which the joint reaches 90% of its range of motion as the end. Similarly for extension, we consider the point where the joint reaches 90% of its range of motion as the start and 10% as the end. These thresholds help to make repeated measurements of an individual consistent where measurement noise or small movements of the joints are not incorrectly identified as the start of an observed flexion or extension.

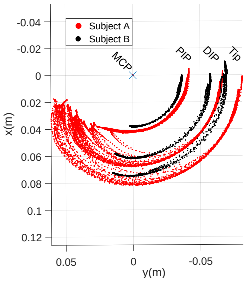

Fig. 3. Joint positions for the index fingers of 2 different subjects while they repeatedly flex their MCP.

The goniometric features extracted can be classified into six categories of joint measurements for both flexion and extension. These include: (1) PIP joint-related measurements, (2) DIP joint-related measurements, (3) MCP joint-related measurements, (4) DIP-PIP interrelationship, (5) PIP-MCP interrelationship, and (6) DIP-MCP interrelationship. The latter 3 feature categories capture how the DIP, PIP, and MCP joints change in relation to each other during finger flexion and extension.

The PIP, DIP, and MCP joint-related measurements each are a set of 12 features (total $3 \times 12 = 36$ features) that capture: (1) the basic statistics of the angle of the joint at various times during flexion and extension (these features pertain to the particular angle that the finer joints make during flexion and extension); (2) the trajectory of the joint during flexion and extension modeled as a quintic function, whose coefficients form the features (which captures both the angles and the broader trajectory of the finger movement); (3) the slope of a linear fit for the trajectory measuring the rate of change of the joint angle during flexion and extension (which represents the speed of the finger motion). Similarly, the DIP-PIP, PIP-MCP and DIP-MCP interrelationship feature categories are a list of 4 features (total $3 \times 4 = 12$ features) each that capture the maximum, median, and average of the ratio of the two joint angles, along with the slope of the linear fit of the scatter plot between the two joint positions during flexion and extension. Together we have a total of 48 $(36 + 12)$ goniometric features.

For the dermatologic features, we primarily measure how much the skin stretches at the proximal and medial phalanges when the finger flexes and extends. At both the phalanges, we extract 5 features, which capture the skin stretch at the beginning and end of the finger movement, the average and median skin stretch, and the skin stretch rate. Together we have a total of 10 (5×2) dermatologic features.

Since all of these features are measured for both the index and middle fingers, we extract a total of $(48 + 10) \times 2 = 116$ features during both flexion and extension of the index and middle fingers. A full list of our features can be seen at: `https://anonymoussubmissionuser.github.io/FeatureList/`.

2.3 Training and Authentication

Once we have the features from the motion-capture of finger flexion and extension, we train an authentication model for each subject in our dataset. The authentication model is a one-vs.-all personalized model for a subject. Subsequently, this model is used in the authentication phase, when a newly captured finger flexion and extension of either finger is evaluated by the model to see if it belongs to the subject.

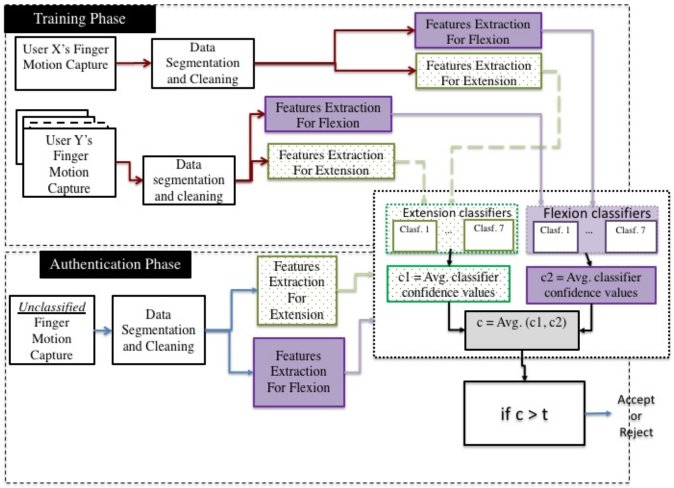
Training Phase
User X's Finger Motion Capture
Data Segmentation and Cleaning
Features Extraction For Flexion
Features Extraction For Extension
User Y's Finger Motion Capture
Data segmentation and cleaning
Features Extraction For Flexion
Features Extraction For Extension
Extension classifiers
Clasf. 1
...
Clasf. 7
Flexion classifiers
Clasf. 1
...
Clasf. 7
c1 = Avg. classifier confidence values
c2 = Avg. classifier confidence values
c = Avg. (c1, c2)
Authentication Phase
Unclassified Finger Motion Capture
Data Segmentation and Cleaning
Features Extraction For Extension
Features Extraction For Flexion
if c > t
Accept or Reject

Fig. 4. Overview of our authentication approach.

Training Phase: During the training phase, we use a portion of our finger motion-capture data to build an authentication model for each subject (we give more details on this in the next section). The training data consists of several iterations of coupled flexion and extension of the PIP and DIP joints and the flexion and extension of the MCP joint as shown in Figure 2 for both the index and middle fingers. For each flexion and it's corresponding extension, we extract a total of 116 features from the motion-capture of the fingers. Once the features are extracted, in order to build an authentication model, we train a *personalized model* for each subject in our dataset. We take the features extracted from the finger movements performed by a particular subject during the training phase as positive class feature points for the subject's personalized model. We then use the features from finger movements performed by all other subjects in our dataset during the training phase as negative class points for the personalized model. These negative class feature points simulate the condition when someone other than the subject, i.e., an adversary, tries to authenticate as the subject. We use both the negative and positive class points for training a machine-learning classifier that acts as the authentication model.

During training we have many more negative feature points than positive feature points. Therefore, we create an ensemble of several classifiers for our authentication model. This is needed to make sure the model does not get biased by the majority class during training. Therefore, instead of one classifier we use a group of 7 classifiers (as we have seven times as many negative feature points than positive feature points), each classifier uses all the positive feature points but using only 1/7th of the negative feature points, which are randomly selected without replacement. Since flexion and extension are two separate types of movements, whose features have different underlying characteristics, we build a total of 14 classifiers (7 that use flexion features and 7 that use extension features). Each of our 14 classifiers outputs a confidence value that describes how confident the classifier is that a new feature point belongs to the subject (whose model is being used). These confidence values from the classifiers are averaged independently for flexion and extension and then averaged again to produce a final confidence value. If this final confidence value is greater than the threshold, t, the model outputs that the new feature point belongs to the subject whose model is being used. All 14 classifiers use the same machine-learning algorithm in our setup.

Authentication Phase: Once the classifiers in the ensemble model are trained using the training data, they can be used to determine whether a new (yet unclassified) flexion and extension movement pair belongs to that subject or not. During the authentication phase, the subject is asked to flex and extend their index or middle finger once (either a coupled flexion and extension of the DIP and PIP joints or a flexion and extension of the MCP joint). The motion-capture system captures the movement and extracts two 116-dimensional features, one for flexion and one for extension. The feature from finger flexion is fed into the 7 classifier ensemble for the flexion features and the feature from finger extension is fed into the 7 classifier ensemble for the extension features. The average of the confidence values of each of these groups of classifiers are then compared against a threshold, t, as described above, to produce the final result that states whether these two new features belong to the subject or not. A diagram of our approach is illustrated in Figure 4.

3 Experimental Setup

In this section we briefly discuss our experimental methodology to evaluate the efficacy of our authentication approach, the choice of machine-learning classifier chosen, and the customization of the feature set for each subject.

Dataset Curation: We obtained an institutional review board (IRB) approval from our university for the data collection. We then recruited eight subjects from the student population for this work. These includes 3 males and 5 females aged 22.1 ± 4.1 years (mean ± std deviation). During data collection we asked each subject to flex and extend their index and middle fingers 10 times in a *session*. We conducted our data collection over two sessions, which we refer to as **session 1** and **session 2**. Session 2 was conducted roughly 1 week after session 1, and data from all subjects were collected in both sessions. For training the models, we used the first 8 iterations of flexion and extension collected from the index and middle fingers for each subject from session 1. We refer to this subset of our dataset as the *training data*. The rest of the flexions and extensions from session 1 and all of session 2 are used to

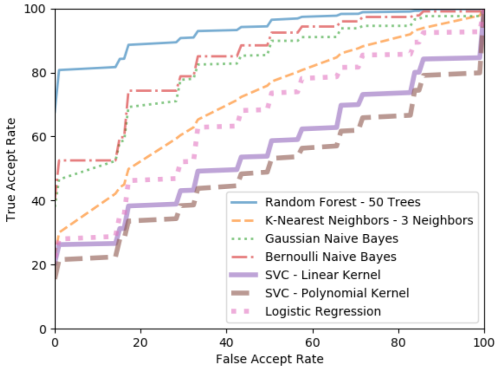

Fig. 5. ROC curves for 5-fold cross validation for various machine-learning classifiers

evaluate the models trained and are referred to as *test data*[2]. The use of data from two sessions allows us to evaluate the performance of our authentication model longitudinally. As the training data consists of eight iterations for IP extension, IP flexion, MCP extension, and MCP flexion collected from index and middle fingers for each subject, there are $(8 \times 4 \times 2) = 64$ movements in each subject's training set. Given the organization of our ensemble model, we split our training data into two different training groups of 32 flexion movements and 32 extension movements, each producing a positive feature point (116-dimensional feature) for our model. In addition, since each subject has their own model, all of the training data from the other subjects in the dataset is used to generate the negative feature points for that subject's authentication model. Therefore, for each subject there are a total of $32 \times 7 = 224$ flexion and 224 extension (116-dimensional) negative feature points.

Metrics: In order to evaluate the efficacy of our approach, we use the following five core metrics. (1) True Reject Rate (TRR): the rate at which true negative feature points (i.e., points from subjects other than the one that the system is trained for) are rejected by the model. (2) False Accept Rate (FAR): the rate at which true negative feature points are accepted by the model. (3) True Accept Rate (TAR) the rate at which true positive feature points (i.e., points from the subject) are accepted by the model. (4) False Reject Rate (FRR): the rate at which true positive feature points are rejected by the model. (5) Equal Error Rate (EER): The rate at which the FAR and the FRR are equal. This is a customary metric in the biometrics/authentication domain and is the point at which our model balances the accuracy of its detection with usability. It can be seen that the highest authentication accuracy ($(TPR + TRR)/2$) of the authentication model is at $1 - EER$.

Classifier Selection: We examine several classifiers for our authentication model, by performing 5-fold cross validation on our ensemble classifier model using the training data. The classifiers that we considered are: Random Forest with 50 trees, K-nearest neighbors with k=3, Gaussian Naive Bayes, Bernoulli Naive Bayes, Support Vector Machine (SVC) with a Linear Kernel, SVC with a polynomial kernel, and Logistic Regression. The reason we chose these classifiers is because of their simplicity and excellent tool support. Ultimately, Random Forest with 50 trees was chosen as it performed the best during cross validation. The Receiver Operating Characteristic (ROC curve) for cross validation of the classifiers can be seen in Figure 5. An ROC curve plots TAR vs. FAR at various operating points of a classifier. The larger the area under the curve, the better the classifier's performance.

Feature Customization: Finally, as subjects are unique, systems are more effective if they are tuned to fit a particular subject [15]. As a result, we use greedy backward feature subset selection (i.e., slowly reduce the number of features used by a model until we reach about half the total number of features) in order to customize the feature set for each individual subject during the training phase. Given that we have 14 classifiers in our authentication model for a subject, we run the feature subset selection for each of the 14 random forest classifiers to produce a customized feature subset for each subject. Figure 6 shows a heat-map of how many of the classifiers, out of the 14 classifier set, for each

[2] We use only the first session's data for training because that's how typical authentication modality works. We enroll (in our case train the model) once and then subsequently authenticate repeatedly.

subject contained a particular feature. The number of classifiers that choose a feature for a subject is written in the corresponding square in the heat map. Further, the larger this number, the darker its coloring. Features are ranked from left to right in descending order of the number of times they were chosen for all subjects. Only features which were chosen by at least three classifiers by every subject are shown in order to highlight the best performing features.

When performing the feature customization, we find that there is great variability in the features selected among the subjects. Several features were selected by a large number of classifiers (13 or 14 classifiers) for a few subjects, but were largely not chosen (i.e., selected by less than 7 classifiers) for other subjects. This indicates that features are fairly unique or personalized to a particular subject or small subset of subjects. For example, feature 68 in Figure 6 is chosen in all 14 classifiers for subject 2, but only chosen in 10 classifiers for subjects 5, and 8, and in 7 or fewer classifiers for the remaining subjects. This indicates that feature 68 is fairly unique to subject 2. Such patterns can be seen in other places in Figure 6 as well, for instance, any column that has a few dark squares are examples of such subject-specific features.

We also found that there were 8 features that performed well in general across all subject models with every subject's model choosing the feature in at least 7 classifiers (50% of the time or more). Those features were (1) *feature 13*: index finger MCP joint angle median; (2) *feature 14*: index finger MCP joint angle average; (3) *feature 11*: index finger MCP joint angle start; (4) *feature 12*: index finger MCP joint angle end; (5) *feature 66*: middle finger PIP joint angle median; (6) *feature 15*: index finger MCP range of motion (10% to 90%); (7) *feature 40*: index finger MCP quintic coefficient a0; and (8) *feature 108*: Proximal skin stretch at 90% range of motion. Since many of these features pertain to the MCP joint on the index finger, this is a joint that we may want to examine in more detail for future work.

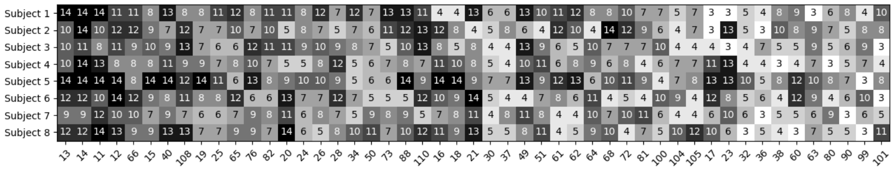

	13	14	11	12	66	15	40	108	19	25	65	76	82	20	24	26	28	34	50	73	88	110	16	18	21
Subject 1	14	14	14	11	11	8	13	8	8	11	12	8	11	11	8	12	7	12	7	13	13	11	4	4	13
Subject 2	10	14	10	12	12	9	7	12	7	7	10	7	10	5	8	7	5	7	6	11	12	13	12	8	4
Subject 3	10	11	8	11	9	10	9	13	7	6	6	12	11	11	9	10	9	8	7	5	10	13	8	5	8
Subject 4	10	14	13	8	8	8	11	9	9	7	8	10	7	5	5	8	12	5	6	7	8	7	11	10	8
Subject 5	14	14	14	14	8	14	14	12	14	11	6	13	8	9	10	10	9	5	6	6	14	9	14	14	9
Subject 6	12	12	10	14	12	9	8	11	8	8	12	6	6	13	7	7	12	7	5	5	5	12	10	9	14
Subject 7	9	9	12	10	10	7	9	7	6	6	7	9	8	11	6	8	7	5	9	8	9	5	7	8	11
Subject 8	12	12	14	13	9	9	13	13	7	7	9	9	7	14	6	5	8	10	11	7	10	12	11	9	13

	30	37	49	51	61	62	64	68	72	81	100	104	105	17	23	32	36	38	60	63	80	90	99	101
Subject 1	6	6	13	10	11	12	8	8	10	7	7	5	7	3	3	5	4	8	9	3	6	8	4	10
Subject 2	5	8	6	4	12	10	4	14	12	9	6	4	7	3	13	5	3	10	8	9	7	5	8	8
Subject 3	4	4	13	9	6	5	10	7	7	7	10	4	4	4	3	4	7	5	5	9	5	6	9	3
Subject 4	5	4	10	11	6	8	9	6	8	4	6	7	7	11	13	4	4	3	4	7	3	5	7	4
Subject 5	7	7	13	9	12	13	6	10	11	9	4	7	8	13	13	10	5	8	12	10	8	7	3	8
Subject 6	5	4	4	7	8	6	11	4	5	4	10	9	4	12	8	5	6	4	12	9	4	6	10	3
Subject 7	4	8	11	8	4	4	10	7	10	11	6	4	4	6	10	6	3	5	5	6	9	3	6	5
Subject 8	5	5	8	11	4	5	9	10	4	7	5	10	12	10	6	3	5	4	3	7	5	5	3	11

Fig. 6. Feature importance heat-map. Feature IDs align with the feature list provided at: https://anonymoussubmissionuser.github.io/FeatureList/.

4 Results

Once the classifiers in our model are chosen and trained, the next step is to see how well the overall authentication model performs. In order to evaluate our models longitudinally, we use as test data the features from finger movements immediately after the training phase (4 flexion/extension combinations from session 1), and from finger movements collected approximately a week later (at least 8 flexion/extension combinations from session 2). For session 2, we had to place the markers on the subject's fingers a second time. However, we did not precisely place the markers in the exact same location as during the training

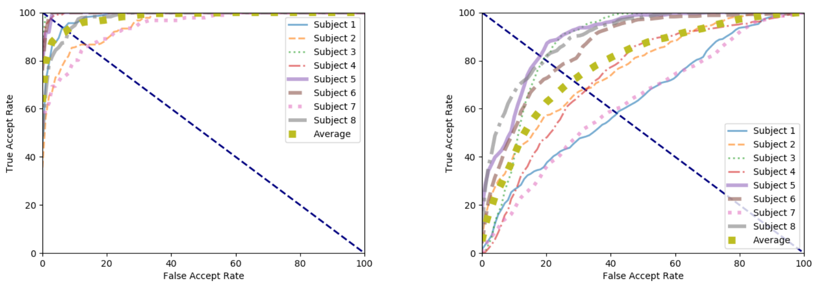

(a) (b)

Fig. 7. ROC curves for (a) session 1 (immediately after training) of test features for all subjects, (b) session 2 (∼1 week later) of test features for all subjects.

phase. This allows us to evaluate the performance of our model in a more realistic setting, longitudinally.

Figure 7(a) shows the performance in session 1 of our models, using the ROC curve, broken down by subject performance. The point where the ROC curve meets the dashed line is the operating point of the authentication model where it reaches EER (lowest error). It can be seen that the accuracy is above the 80% mark, approaching the dashed line for even the worst performing subjects, with near-perfect performance on some subject models. The authentication accuracy is lower in session 2 compared to session 1 as seen in Figure 7(b). This is due to both the inconsistent placement of the markers as well as the duration of time since training. The average EER rates for session 1 was 6.3% and session 2 was 16.7%. Even though we present the results in terms of EER, the advantage of showing the ROC curves is that we can see what happens if we optimize the thresholds to shift the balance to favor false acceptance or false rejection, depending on the needs of the system being deployed. In many cases it could be argued that we minimize false accepts at all costs while tolerating higher false rejects (i.e., entrance to a secure facility), while for others we do the opposite (i.e., entrance to a commercial building).

Given these results, we then evaluated which of the two movement types we used in this work (i.e., coupled PIP-DIP flexion/extension or MCP flexion/extension) worked better during the authentication phase. Figure 8(a) shows the result in the form of the ROC curve. It can be seen that the overall difference between the two types of movement was largely nonexistent, with MCP flexion/extension performed better than coupled PIP-DIP flexion/extension immediately after training, while the latter performed better longitudinally. We also evaluated which of our two fingers was better in the authentication phase, given the trained models. As can be seen from the average ROC curves over all subjects in Figure 8(b), the movement of the middle finger seems better at identifying a subject than the index finger.

However, overall it is clear that the motion-capture of finger movement and using fingers to capture the biomechanics of finger movements have the potential to uniquely identify an individual over time. Furthermore, the ability of the approach to authenticate based off of unseen test data shows that the system is effective even over natural variation in joint angles and motions during repetition. In the future, we plan to use larger datasets to explore these results in more detail, develop methods to reduce the longitudinal error rate of the authentication models, and explore methods for identifying joint centers and angles *without the use* of adhesive markers.

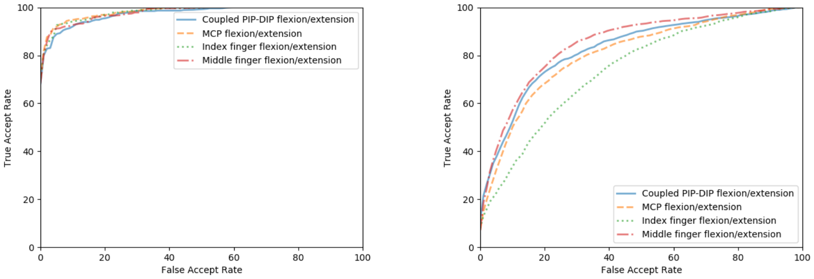

(a) (b)

Fig. 8. Average ROC curve over all subjects for PIP-DIP and MCP flexion/extension, and index finger movement and middle finger movement for: (a) session 1 and (b) session 2.

5 Related Work

There has been a wide variety of interest in finger related biometrics in recent years. This includes biometrics based on: keyboard dynamics [13], in-air signatures [4], gestures [16], knuckle pattern [5], and fingerprint [10]. However, all of these approaches look at either the hand itself or focus on actions performed by the hand when accomplishing a particular task. They do not focus on the movement characteristics of the individual fingers, which, as we have shown, are themselves unique.

In [14] the authors utilize a cyber-glove [1] to measure joint angle changes while a person manipulates an object as a way to identify a subject. The premise behind the work is that the way that people handle objects is inherently unique, and that joint angles can be used to measure the person-object interaction. In addition to the grasping action other work often also tracks arm movement during the grasp [11], in addition to image analysis of the hand position during and after the grasp [6]. Compared to all of these approaches our work operates based on the biomechanics of the fingers by applying just the movement of the fingers without the use of any props.

6 Conclusion

In this paper we presented a novel authentication system based on biometrics derived from the biomechanics of fingers using a marker-based motion-capture system. Specifically, we focused on the flexion and extension movements of the index and middle fingers. We built personalized authentication models for subjects using goniometric and dermatologic features extracted via motion-capture and evaluated their performance longitudinally. This is a preliminary work intended to show the viability of this approach. In the future, we plan to extend this work in several ways: (1) deploying this system for visually impaired subjects with different finger sizes, genders, and age groups; (2) perform more stringent security analysis where adversaries try to copy a victim's finger movement; and (3) explore marker-less methods for capturing finger movement for authentication.

Acknowledgments

The authors would like to thank Tess Meier who helped with the data collection for this work. This work is supported by the defense health program grant DHP W81XWH-15-C-0030.

References

1. CyberGlove Systems. http://www.cyberglovesystems.com/
2. Opitrack. http://optitrack.com/
3. The Braille Literacy Crisis in America. https://nfb.org/images/nfb/documents/pdf/braille_literacy_report_web.pdf
4. Behera, S.K., Kumar, P., Dogra, D.P., Roy, P.P.: Fast signature spotting in continuous air writing. In: Machine Vision Applications (MVA), 2017 Fifteenth IAPR International Conference on. pp. 314–317. IEEE (2017)
5. Choraś, M., Kozik, R.: Contactless palmprint and knuckle biometrics for mobile devices. Pattern Analysis and Applications **15**(1), 73–85 (2012)
6. Drosou, A., Ioannidis, D., Tzovaras, D., Moustakas, K., Petrou, M.: Activity related authentication using prehension biometrics. Pattern Recognition **48**(5), 1743–1759 (2015)
7. Gamage, N., Kuang, Y.C., Akmeliawati, R., Demidenko, S.: Gaussian process dynamical models for hand gesture interpretation in sign language. Pattern Recognition Letters **32**(15), 2009 – 2014 (2011)
8. Gupta, P., Gupta, P.: Multi-biometric authentication system using slap fingerprints, palm dorsal vein and hand geometry. IEEE Transactions on Industrial Electronics pp. 1–1 (2018)
9. Lee, T.: Biometrics and disability rights: Legal compliance in biometric identification programs. Journal of Law Technology and Policy **2016**(2), 209 – 244 (2016)
10. Marasco, E., Ross, A.: A survey on antispoofing schemes for fingerprint recognition systems. ACM Computing Surveys (CSUR) **47**(2), 28 (2015)
11. Patel, V., Thukral, P., Burns, M.K., Florescu, I., Chandramouli, R., Vinjamuri, R.: Hand grasping synergies as biometrics. Frontiers in bioengineering and biotechnology **5**, 26 (2017)
12. Tagkalakis, F., Vlachakis, D., Megalooikonomou, V., Skodras, A.: A novel approach to finger vein authentication. In: 2017 IEEE 14th International Symposium on Biomedical Imaging (ISBI 2017). pp. 659–662 (2017)
13. Teh, P.S., Teoh, A.B.J., Yue, S.: A survey of keystroke dynamics biometrics. The Scientific World Journal **2013** (2013)
14. Vogiannou, A., Moustakas, K., Tzovaras, D., Strintzis, M.G.: A first approach to contact-based biometrics for user authentication. In: International Conference on Biometrics. pp. 838–846. Springer (2009)
15. Wobbrock, J.O., Kane, S.K., Gajos, K.Z., Harada, S., Froehlich, J.: Ability-based design: Concept, principles and examples. ACM Transactions on Accessible Computing (TACCESS) **3**(3), 9 (2011)
16. Wu, J., Christianson, J., Konrad, J., Ishwar, P.: Leveraging shape and depth in user authentication from in-air hand gestures. In: Image Processing (ICIP), 2015 IEEE International Conference on. pp. 3195–3199. IEEE (2015)